BRAIN
ORIGINAL ARTICLE

Travelling waves reveal a dynamic seizure source in human focal epilepsy

Joshua M. Diamond,[1] Benjamin E. Diamond,[2] Michael S. Trotta,[1] Kate Dembny,[3] Sara K. Inati[3] and Kareem A. Zaghloul[1]

Treatment of patients with drug-resistant focal epilepsy relies upon accurate seizure localization. Ictal activity captured by intracranial EEG has traditionally been interpreted to suggest that the underlying cortex is actively involved in seizures. Here, we hypothesize that such activity instead reflects propagated activity from a relatively focal seizure source, even during later time points when ictal activity is more widespread. We used the time differences observed between ictal discharges in adjacent electrodes to estimate the location of the hypothesized focal source and demonstrated that the seizure source, localized in this manner, closely matches the clinically and neurophysiologically determined brain region giving rise to seizures. Moreover, we determined this focal source to be a dynamic entity that moves and evolves over the time course of a seizure. Our results offer an interpretation of ictal activity observed by intracranial EEG that challenges the traditional conceptualization of the seizure source.

1 Surgical Neurology Branch, NINDS, National Institutes of Health, Bethesda, MD 20892, USA
2 J.P. Morgan AI Research, Corporate and Investment Bank, JP Morgan Chase & Co., New York, NY 10017, USA
3 Clinical Epilepsy Section, NINDS, National Institutes of Health, Bethesda, MD 20892, USA

Correspondence to: Kareem A. Zaghloul
Surgical Neurology Branch
NINDS, National Institutes of Health Building 10, Room 3D20, 10 Center Drive Bethesda, MD 20892-1414, USA
E-mail: kareem.zaghloul@nih.gov

Correspondence may also be addressed to: Sara K. Inati
Office of the Clinical Director
NINDS, National Institutes of Health, Building 10, Room 7-5680, 10 Center Drive Bethesda, MD 20892-1445, USA
E-mail: sara.inati@nih.gov

Keywords: epilepsy; seizure; localization; computation; iEEG

Abbreviations: EI = epileptogenicity index; iEEG = intracranial EEG

Introduction

Surgical treatment of patients with drug-resistant focal epilepsy relies upon accurate localization of the brain region that gives rise to seizures. For decades, the clinical gold standard for localizing this region has been the identification of the seizure onset zone using intracranial electroencephalography (iEEG) recordings. The seizure onset zone is traditionally identified by visual inspection of the earliest changes in iEEG traces or by identification of focal high-frequency activity at seizure onset.[1–7] This has guided treatment for each individual patient and shaped our understanding of the spatial and temporal evolution of focal seizures in humans.

While a number of iEEG patterns of activity have been described at seizure onset, including the classic finding of low

Received August 17, 2020. Revised December 08, 2020. Accepted December 23, 2020. Advance access publication March 9, 2021

voltage fast activity, as the seizure progresses, ictal activity frequently evolves to consist of more spatially distributed low-frequency large-amplitude rhythmic fluctuations.[2–4,8,9] Brain regions demonstrating these low frequency rhythms have traditionally been assumed also to be actively seizing.[10–12] Recent evidence, however, has questioned this interpretation. Neuronal firing is typically expected to increase and become intensely hypersynchronous during a seizure. This has not consistently been observed in brain regions involved in these rhythms.[9,13–18] An alternate interpretation suggests that this activity may instead reflect propagated barrages of pathologic activity emitted from a relatively focal seizure source.[9,17,19–22] This activity may rapidly propagate over white matter pathways, or it may spread across the cortical sheet in the form of travelling waves.[9,14,17,19–24] Such pathological travelling waves may not require synaptic transmission[25] and may lead to widespread abnormal iEEG activity as well as disruption of normal cortical function and clinical symptoms.

The possibility that areas of active seizure are confined to a relatively focal region is supported by recent studies of human epilepsy examining phase-locked high gamma activity.[26,27] This pattern of iEEG activity is highly correlated with regions that are actively seizing on microelectrode recordings, appears to remain more focal than observed ictal rhythmic patterns and spreads slowly over spatial scales at a rate similar to that of the ictal wavefront[9,14] and to the progression of clinical symptoms observed during the Jacksonian march. In fact, although the presence of a focal seizure source is a fundamental principle underlying the success of resective surgery for epilepsy, the use of intracranial recordings to identify seizure foci may rest implicitly on the assumption that seizures demonstrate some degree of local spread prior to widespread propagation. Clinical iEEG implantations are planned rigorously using non-invasive testing and semiology to target specific brain regions. However, it is likely that a typical implantation only records from a small percentage of the brain's surface area. Prior research has suggested that the spatial radius of the LFP is about 200 μm,[28] compared to a typical neocortical surface area of about 2400 cm^2.[29] Therefore, even given optimal planning prior to implantation, and correct pre-implantation hypotheses, the electrodes are likely to record locally propagated rather than direct ictal activity, particularly early in the seizure.

Here, in a group of participants with focal epilepsy, we observed that rhythmic activity occurring during the evolution of seizures appears in different electrode contacts with different time delays. These observations are consistent with the presence of travelling waves of activity emitted from a relatively focal source, which then propagate over the cortical sheet. We therefore created a simple model that can account for these observations and performed source localization using techniques that have been established in fields such as acoustics, radar and geophysics.[30–36] One such method, phase multilateration, utilizes phase differences at adjacent sensors to localize a distant source.[37] Here, we adapted this method to estimate the source of observed rhythmic ictal activity and found that our model produces accurate estimates for the location of the seizure source and may be sufficient to explain much of the activity recorded during seizures. We found that the estimated sources of these travelling waves change locations over the course of individual seizures, often with a stereotyped pattern of migration that is conserved across seizures within individual patients. In addition, our initial localizations matched those identified using standard neurophysiologically based localization methods such as the epileptogenicity index (EI) and phase-locked high gamma activity, while also matching the location of the resection territory in patients with good seizure outcomes. Our data therefore support recent work suggesting that actively seizing cortex, as defined by rapid, hypersynchronous neuronal firing, may remain more focal than has traditionally been appreciated.

Materials and methods

Participants

Twenty participants underwent a surgical procedure for placement of intracranial electrodes followed by iEEG monitoring in anticipation of a surgical resection for drug-resistant epilepsy. We performed all surgical procedures and iEEG monitoring at the Clinical Center at the National Institutes of Health (Bethesda, MD). In each case, the clinical team determined the placement of the contacts to localize epileptogenic regions. Each participant had at least 1 year of follow-up and the outcome was evaluated using the Engel class.[38] The research protocol was approved by the Institutional Review Board, and informed consent was obtained from the participants. Data were analysed using custom MATLAB scripts (Mathworks). All data are reported as mean ± standard deviation (SD) unless otherwise reported.

Source localization

Previous evidence has motivated an emerging hypothesis that posits that, in patients with focal epilepsy, there is a focal source of seizure activity that releases propagating waves, which are then detected by electrode contacts.[9,17,19–22] Under this hypothesis, it is unlikely that any single electrode contact is recording directly from the source of seizure activity. Rather, electrodes capture waves that propagate from the source over the cerebral cortex. Each electrode serves as a sensor participating in signal receipt. We may then use these signals to estimate the center of mass of a focal area of seizure activity by examining differences in the signal recorded by nearby electrodes. In our model, we assume that a signal emitted by the source spreads outward in a circular manner over the cortical surface of the brain, represented in our work as a geodesic mesh.[22] Our approach has been used extensively for signal detection in acoustics and radar[30–33,39] and for earthquake epicentre detection in geophysics.[34–36,40,41] In fact, many models for earthquake localization—the so-called '1-dimensional models'—likewise assume a uniform speed of outward propagation given any particular depth below the earth's surface.[35,40,41] However, we acknowledge that, in brain tissue, the uniform outward spread of a signal is a simplifying assumption for the purposes of computation, which may not be faithful to the underlying properties of the tissue. This assumption may lead to inaccuracy in our model, because it disregards the possibility of non-uniform spread, caused by non-local interactions along different brain pathways such as the white matter (Supplementary material).

Consider a single source, s, which emits a wave of activity that is detected by a single electrode, e_i. The time between the emission of the signal by s and its receipt at electrode e_i is governed by the distance between them, d_{s,e_i} and by the speed of the emitted wave, c, through the simple expression, $d_{s,e_i} = c \cdot \tau_i$, where τ_i denotes the time delay required for electrode e_i to receive the wave. Previous work in humans with epilepsy has found that travelling waves have a speed of ∼300 mm/s, which we used for our estimate of speed here in all participants and seizures.[9,16,19,20] We confirmed that travelling waves propagate at ∼300 mm/s in our dataset (Supplementary material).

In practice, the location of the source, and therefore the distance between the source and any single electrode, d_{s,e_i}, as well as the time delay τ_i, is unknown. However, by using the difference in time delays with which wave activity is received at two distinct electrodes, we can produce an expression for the difference in

distances between the source and the two electrodes. Consider a second electrode contact, e_j, that detects activity propagated from the same source. If electrode e_i is closer to the source s than electrode e_j, then the delay between emission and receipt at e_i will be less than same time delay at e_j, such that $\tau_i < \tau_j$. Note that as a first approximation, we assume that propagated wave activity travels with a uniform speed through the tissue to all electrode contacts and that any differences in time of receipt reflect only the distances between the source and the electrodes (Supplementary material). We can therefore express the difference in distances between the source and these two electrodes as follows:

$$d_{s,e_i} - d_{s,e_j} = c \cdot (\tau_i - \tau_j). \quad (1)$$

The relative distance between the source and the two electrodes can therefore be expressed using the difference in time delays $\tau_i - \tau_j$ required for the signal to propagate from the source to the two electrodes (section 3.9 in Munoz *et al.*[39]).

Previous evidence has suggested that the seizure source emits oscillatory propagating waves.[4,9,16,19] Given the oscillatory nature of this signal, we can use the phase difference between the signals observed at electrode pairs as a surrogate for the difference in time delays (Fig. 1B). The use of phase to estimate time delays is preferable because it allows us to infer the location of the source at every single time point. Moreover, even if the dominant frequency of the oscillatory signal changes, the commensurate change in the relative phase difference measured over adjacent sensors would still translate to the same time delay (Supplementary material). For the purposes of source localization, we assume that the iEEG signal recorded at an electrode represents signal propagated from the source, although the activity recorded at each electrode likely reflects interactions between propagated activity and local circuitry.

Consider that the source begins emitting waves at time $t = 0$, with an initial phase equal to φ_0. The phase of a wave recorded at electrode e_i, at the present time t, is given by the phase of the wave at the source at the present time minus the transit time, $t - \tau_i$, and by the frequency of the wave, f (section 1.3 in Boashash[42]):

$$\varphi_i(t) = 2\pi \cdot f \cdot (t - \tau_i) + \varphi_0. \quad (2)$$

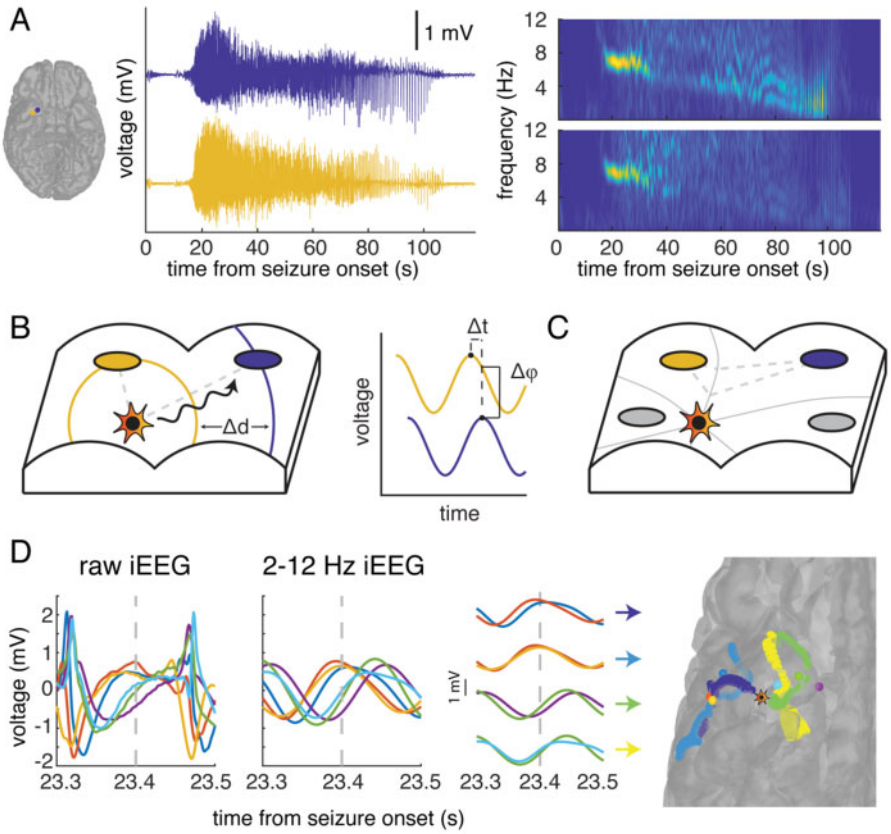

Figure 1 The source of seizure activity emits travelling waves. (**A**) In a typical seizure event recorded by two electrodes (blue and yellow) in the inferior temporal lobe in a single participant, the iEEG recording demonstrates an initial period of high-frequency activity that transitions to a characteristic low-frequency, high-amplitude periodic spike-and-wave pattern. A spectrogram of the iEEG recordings in both electrodes (*right*) demonstrates the emergence of a single dominant frequency band at around 20 s after seizure onset, which reflects the oscillatory nature of the recorded signal. The frequency of this signal progressively decreases with time. (**B**) We hypothesize that there is a single source of seizure activity (star) that emits travelling waves (black). In a schematic representation of a section of cortex, these waves propagate in a circular manner and are detected by different iEEG electrodes (blue and yellow) at different times. We use the difference in phase of the waves recorded at adjacent electrodes (*right*) as a surrogate for the difference in time in order to compute the relative difference in distance between the source and each electrode. (**C**) The relative difference in distance (grey dashed line) between the source and two electrodes, computed using the difference in phases of the recorded oscillatory signal, constrains the location of the source of activity to a point on a hyperbola (grey solid line). With multiple pairs of electrodes, we produce multiple hyperbolae at each time point of seizure activity. We estimate the location of the source (star) as the point that lies closest to the intersection of the hyperbolae. (**D**) The raw (*left*) and 2–12 Hz filtered (*middle*) iEEG signal recorded by six electrodes in the same example participant demonstrates the spike-and-wave morphology and respective phase differences between the electrode signals. The colour of the electrode's trace is preserved across panels. Using the phase difference over pairs of adjacent electrodes, we may generate hyperbolae on the cortical surface (*right*, coloured for each pair) that constrain the estimated location of the source of the emitted waves (star) at each single sample, in this case 23.4 s following seizure onset (grey dashed line).

At each time point in each electrode, we can measure the instantaneous phase, $\varphi_i(t)$. Before source localization, our raw signal is bandpass-filtered at 2–12 Hz (Supplementary material). As a first approximation, we assume that the source is stationary or slow moving, and that the frequency of the waves emitted by the source changes slowly over time and does not change as it travels through tissue. Thus, we take the frequency f to be a global constant (see Supplementary material for further consideration). Using the relative differences in instantaneous phase between two electrodes rather than the time delay, we can now express the relative difference in distance between the source and the two electrodes, e_i and e_j, at every time point, t, as a function of the difference in their instantaneous phases:

$$d_{s,e_i}(t) - d_{s,e_j}(t) = -\frac{c}{2\pi \cdot f}\left(\varphi_i(t) - \varphi_j(t)\right). \quad (3)$$

At each time point, t, we can therefore compute the relative distance between the source and the two electrodes using only the phase information that is available to us at that particular time.

The set of points whose respective distances from two electrodes differ by a constant defines a single branch of a hyperbola. Thus, having ascertained a difference in time delay or phase, we may narrow the location of the source to a branch of a hyperbola in two dimensions. With multiple pairs of electrodes, we can produce multiple hyperbolae, and therefore estimate the location of the source as the single point that most closely matches the intersection of those hyperbolae.

In order to use the difference in phase detected at two electrodes to estimate the location of the source, each electrode pair must satisfy constraints regarding the distance between them (<12 mm), their relative frequencies, and their overall power with respect to all other electrodes at that time point (Supplementary material). At every time point, we use every electrode pair (e_i, e_j) that satisfies our constraints to construct a solution set for the location of the source, $H_{ij}(t)$. This solution set is a single branch of a hyperbola in the geodesic space, defined by the computed relative difference $d_{s,e_i}(t) - d_{s,e_j}(t)$. The hyperbola is defined such that the difference in distance from each point on the hyperbola to the two electrodes is fixed. $H_{ij}(t)$ is limited to the vertices of the cortical geodesic mesh, since seizure activity can only originate in grey matter. Because the number of cortical vertices is finite, we allow a margin of error of 0.5 mm above or below the expected relative distance to produce $H_{ij}(t)$. Additionally, any propagating waves that are reliably detected at each electrode are unlikely to have been emitted from a source that is far away, and so we limit each solution set such that all points in the set $H_{ij}(t)$ that are no greater than 30 mm from either electrode in geodesic distance.

With multiple eligible pairs of electrodes, we may generate multiple hyperbolic solution sets at each time point. The problem of source localization is under-determined if we use fewer than three electrode pairs, and so at every time point we only estimate the location of the source if a minimum of four electrode pairs from the same hemisphere satisfy our constraints. We use the hyperbolae generated from these electrode pairs to estimate the location of $\hat{s}(t)$, the source of wave activity at every time t. To do so, we identify the single vertex that minimizes the sum of the squared distances between that estimated source location and each solution set. For each solution set H, the minimum distance between some source point s and that solution set is denoted with $d_{s,\ H}$. Because it is computationally expensive to compute the geodesic distance between every possible vertex that can be assigned to a hyperbola and every other possible vertex in the cortical mesh, we use Euclidian rather than geodesic distance to compute $d_{s,\ H}$. We also require that the source vertex which is ultimately discovered is within 30 mm of at least one participating electrode pair.

The best estimate of source location at each time point, $\hat{s}(t)$, is then given by:

$$\hat{s}(t) = argmin_s \sum_{(e_i,e_j)\in P(t)} d^2_{s,H_{ij}(t)} \quad (4)$$

where $P(t)$ is the set of electrode pairs at time t that satisfy our constraints (Supplementary material). At every time point, we thus estimate the location of the source of activity, $\hat{s}$. During any one second of a seizure, it is possible to identify up to 1000 source points, one for each sample. In practice, however, not every time point will have a sufficient number of electrode pairs that satisfy our constraints, and the number of source points identified is often less than 1000 per second.

Data availability

Simulated data and custom MATLAB analysis code for estimating source locations used for the current study can be found at: https://dir.ninds.nih.gov/ninds/zaghloul/downloads.html (accessed 15 April 2021).

Results

We examined iEEG recordings in 20 participants (36.60 ± 10.84 years old; nine females) with drug-resistant epilepsy who were monitored for seizures with subdural and depth electrodes (Table 1). Participants in this cohort experienced focal seizures, with or without secondary generalization, during the monitoring period. Each participant had, on average, 6.2 ± 4.2 seizures, for a total of 123 seizures over all participants. The mean seizure length was 261.47 ± 135.01 s per participant (mean ± 95% confidence interval). Of the 20 participants, 14 achieved an Engel Class 1 outcome following surgical resection, and two each achieved an Engel 2, 3 and 4 outcome. For the purposes of analysis, we divided our participants into those with good seizure outcome (Engel 1; 14 participants) and those with poor seizure outcome (Engel 2 or greater, six participants).

In a typical seizure event, we observed a brief period of high-frequency activity captured soon after seizure onset (Fig. 1A). Consistent with previous reports, this typically transitions to a characteristic low-frequency, high-amplitude periodic spike or spike-and-wave pattern.[2–4,8,9,20] A spectral decomposition of the iEEG trace from two electrodes demonstrates that this transition is marked by a single dominant band that decreases in frequency over time, indicating a strong oscillatory component between 2–12 Hz.

The oscillatory spike and spike-and-wave pattern observed during a typical seizure motivates a simple model in which a focal source of seizure activity emits periodic travelling waves that are then detected by electrode contacts. In this model, each electrode may receive travelling waves at different times, depending on its distance from the source of activity (Fig. 1B). Because the observed patterns of recorded activity are oscillatory, we may use the difference in phase between the detected waves at adjacent electrodes as a surrogate for the difference in distance between each electrode and the source of activity (see 'Materials and methods' section). A fixed difference in distance between the hypothesized source of activity and two electrodes constrains the possible location of the source to a hyperbola. With multiple pairs of electrodes, and therefore multiple measures of the phase difference, we can produce multiple hyperbolae and estimate the location of the seizure source as the intersection between them (Fig. 1C; see 'Materials and methods' section).

In the same example participant, we filtered the raw iEEG data into the 2–12 Hz band and examined the phase difference between adjacent pairs of electrodes (Fig. 1D) (see 'Materials and methods' section and Supplementary material). We used the relative phase differences between multiple electrode pairs to construct multiple

Table 1 Patient demographic information

Patient ID	Sex	Age	Seizure type	MRI	Procedure	Pathology	Engel class
1	F	33	FIAS, F2BTCS	NL	L lateral temporal topectomy	MDG	2b
2	F	30	FIAS	NL	L SAH	HS, MDG	2b
3	F	59	FIAS	L MTS	L ATL	HS	1a
4	F	49	FIAS, F2BTCS	L MTS	L SAH	HS	3a
5	M	45	FIAS, F2BTCS	NL	R F topectomy	MDG	1a
6	M	33	FIAS, F2BTCS	NL	L ATL	MDG	3a
7	F	35	FIAS, F2BTCS	Possible B MTS	L ATL	HS, MDG	1a
8	M	33	FIAS, F2BTCS	B PVNH	L ATL	MDG	1a
9	F	28	FIAS	L MTS	L ATL	HS, MDG	1b
10	F	30	FIAS	R P encephalo-malacia, R MTS	R ATL	HS	1b
11	M	34	F2BTCS	NL	R P topectomy	MDG	2b
12	M	27	Focal, some lesionectomy	electrographic LGG	L LT LGG 1a	L T	
13	M	29	FAS, F2BTCS	NL	R P topectomy	MDG	4b
14	M	32	FIAS, F2BTCS	B PVNH	L ATL	MDG	1a
15	F	33	FIAS	R F FCD	R F lesionectomy	FCD	1a
16	M	21	FIAS, F2BTCS	NL	R ATL	MDG	1a
17	M	26	FIAS, F2BTCS	NL	L F topectomy	FCD	1a
18	M	57	FIAS, F2BTCS	R T encephalocele	R ATL	MDG	1a
19	F	53	FIAS	NL	R ATL	HS, FCD	1b
20	M	45	FIAS	R > L perisylvian polymicrogyria	R ATL	HS, MDG	1b

ATL = anterior temporal lobectomy; B = bilateral; F = frontal; F2BTCS = focal to bilateral tonic-clonic seizures; FCD = focal cortical dysplasia; FIAS = focal impaired awareness seizure; HS = hippocampal sclerosis; L = left; LGG = low-grade glioma; MDG = microdysgenesis; MTS = mesial temporal sclerosis; NL = no lesion; P = parietal; PVN = periventricular nodular heterotopia; R = right; SAH = selective amygdalohippocampectomy; T = temporal.

hyperbolae. We then estimated the location of the source of the emitted waves by finding the point on the cortical surface that lies closest to the intersection of these hyperbolae. The estimated source location does not lie immediately near any one electrode, suggesting that the travelling waves may be used to localize even a distant source.

The seizure source moves over short and long timescales

Previous research in the clinical setting as well as in *in vivo* and *in vitro* models of epilepsy has suggested that the source of seizure activity is capable of slowly changing locations over the course of a seizure.[8,9,15,16,18,22] The seizure source may remain a single focus of activity that changes location, or the seizure may recruit more brain regions that collectively act as a larger source of activity that appears to occupy a new location. If the source is emitting travelling waves that are detected by the recording electrodes,[8,9,14,20] then we should observe evidence of such movement in the iEEG traces.

In the same example seizure event, a magnified view of the initial time period following the transition to spike-and-wave activity reveals the relative phase differences between the activity recorded in both electrodes (Fig. 2A). Notably, the phase relationship between the two electrode recordings changes with time and reverses ~23–24 s following the onset of the seizure. Similar reversals in the phase relationship between electrodes have previously been observed.[9,16] This reversal suggests that the source of the emitted travelling waves may initially start closer to one electrode, then reach a point that is equidistant to the two electrodes, before becoming closer to the second. If the phase difference between two electrodes changes, then the hyperbola used to estimate the location of the source of the emitted waves will also change (Fig. 2B; see 'Materials and methods' section). In the same example seizure event, the hyperbola corresponding to the phase difference observed in the two electrodes initially curves towards the lateral electrode (Fig. 2C). At a later time point when the phase relationship between the electrode reverses, the hyperbola curves towards the medial electrode. Because the phase differences between electrode contacts are relatively stable over several hundred milliseconds, there is no change in the shape of the extracted hyperbolae over millisecond timescales.

We computed the phase difference between multiple electrode pairs at every time point during this seizure and counted the number of times the seizure source was estimated to lie in each brain region of interest during each 1-s epoch (Fig. 2D). Over three sample 1-s epochs spanning 8 s, we found that the estimated location of seizure activity moves from the anterolateral to the medial subtemporal cortical surface. Using the phase differences between electrode pairs at every time point, we were able to observe the progressive transit of the seizure source over the cortical surface with time.

We next examined the temporal evolution of the seizure source over the entire course of this seizure. We coloured each location by the time in the seizure at which that location was estimated to be the seizure source (Fig. 3A). We were also interested in where the estimated location of the seizure source lay with respect to the location of the resection that was subsequently performed, shaded in black. During this same seizure event, the estimated seizure source first briefly localized to the left subtemporal cortex, then migrated to the right anterior lobe, then to the right lateral temporal lobe and finally briefly returned to the left lateral temporal cortex. Consistent with previous observations, these results suggest that the source of seizure activity may migrate and occupy several distinct foci over the course of a seizure.[8] During three

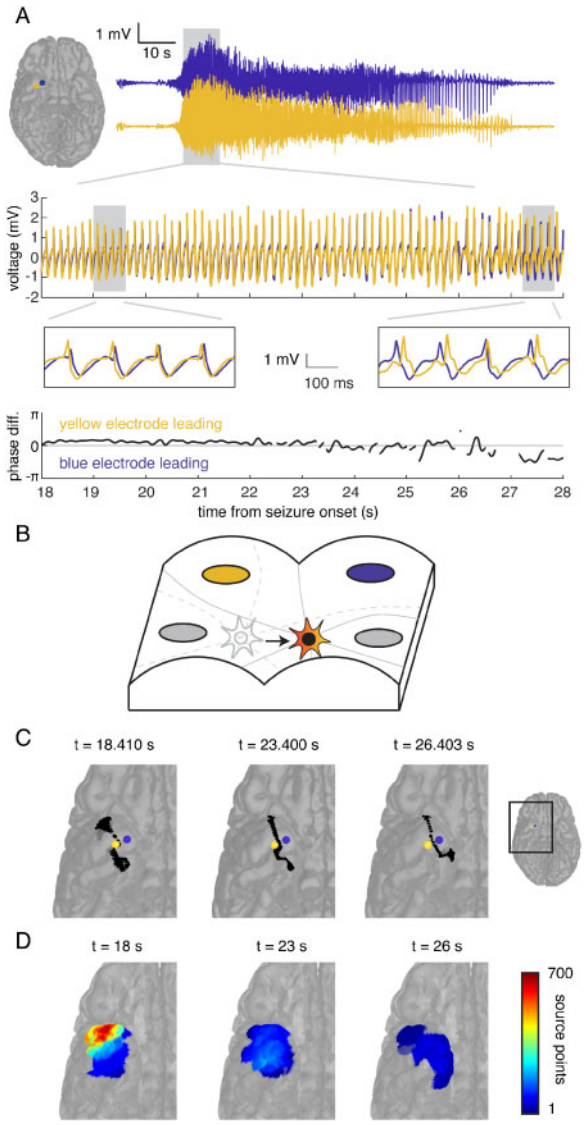

Figure 2 The estimated location of the source of seizure activity changes with time. (**A**) A magnified view of 10 s of the iEEG time series data (*top, middle insets*) recorded by two electrodes demonstrates the phase relationship between the tracings recorded by both electrodes (*bottom*). Initially, activity in the lateral electrode (yellow) leads activity in the medial electrode (blue, *left inset*), but this phase relationship reverses around 23 s following the onset of the seizure (*right inset*). (**B**) Using the phase difference between the signals recorded in each pair of electrodes generates a hyperbola (grey) for each pair that constrains the estimated location of the source of seizure activity at every time point. If the phase differences change over time, the hyperbolae, and therefore the estimated location of the source, also change, suggesting that the source of the emitted waves is moving (grey to red star). (**C**) For the two example electrodes, the hyperbola (black) that estimates the location of the source on the reconstructed cortical surface initially curves towards the lateral electrode (yellow), but then curves towards the medial electrode (blue) at a later time point. (**D**) We aggregated the number of times any location was estimated as the source of the emitted waves into regions of interest during each 1-s epoch. Each region of interest is coloured according to the number of times a point within that region of interest was estimated as the seizure source during that 1-s epoch. Over three epochs, the location most frequently estimated as the seizure source moves from the anterolateral to medial subtemporal cortex.

additional seizures in the same participant (Fig. 3B), we observed a similar stereotyped pattern of seizure source movement, suggesting that patterns of seizure origin and spread are conserved within individual participants across different seizures.[3,14,15,20]

In the same example seizure, we calculated the rate of localization for each region of interest, defined as the number of times the estimated source localizes to each region of interest during every second of each seizure. This rate can change from moment to moment, and over the course of an individual seizure, each region of interest will have its own peak rate of localization that occurs at some time point in that seizure. For each region of interest, we identified the maximum rate observed up to and including three different time points during the seizure (Fig. 3C; for all participants, see Supplementary Fig. 1). As the seizure progressed in time, the regions of interest containing the greatest rate of localization were located in the anterior temporal lobe. Even during later time points in the seizure when the source was estimated to lie in the lateral temporal cortex, the rate of localization did not exceed the initial rates of localization in the anterior temporal lobe. In this participant who achieved seizure freedom following surgical resection, the region of greatest detection rate also lay within the resection cavity.

The rates of localization suggest that robust early source localization can be more focal than estimates that are generated during later time points in the seizure. To more clearly visualize this in four seizures in this participant, we collapsed the locations of the estimated source across the superior-inferior and left-right dimensions and retained only the anterior-posterior dimension, plotted against time (Fig. 3D). In all four seizures, robust source detection arose in the anterior temporal lobe within the resection cavity at around 15–20 s after seizure onset. Notably, in all three seizures the estimated location of the seizure source then became more diffuse and less consistent, appearing to migrate posteriorly.

We quantified the degree of spatial spread of our localized source points to determine the extent to which source localization becomes more focal or diffuse over time. During every second of every seizure, we computed the centroid of the discovered source points. We then computed the mean Euclidean distance from each source point discovered during that second to the corresponding centroid. This calculation is akin to the standard deviation in three dimensions. Across all seizures in this participant, we found that the average measure of spatial spread was significantly smaller during the first 30 s compared with the next 30 s of seizure [3.97 ± 2.06 versus 6.88 ± 2.33; $t(5) = 8.28$, $P = 0.0004$, paired *t*-test; Fig. 3E, left]. We repeated this analysis for all participants, and across participants again found that the spatial spread during the first 30 s was significantly smaller than the next 30 s [4.94 ± 1.46 versus 6.35 ± 2.15; $t(17) = 2.98$, $P = 0.008$, paired *t*-test; Fig. 3E, right]. This suggested that the source expands over time. We then examined the extent to which the location of the source changes over the course of a seizure. We computed the mean location of all centroids during the first 30 s of a seizure and compared that to the mean location during the second 30 s. Across participants, the average difference in spatial location across seizures was 17.88 ± 12.91 mm, substantially greater than the spatial spread. In addition, we found that the maximal distance between all centroids, averaged over all participants, was 77.10 ± 23.28 mm. Together, these data suggested that the focal source of seizure activity may become more diffuse with time or may expand (Supplementary Figs 1, 3 and 4), but that the movement of the centroid of source activity may exceed the expansion.

The seizure source emerges from early high frequency activity

An established clinical approach for identifying the seizure onset zone using iEEG is to identify electrodes that exhibit early onset of high-frequency activity. One measure of such high-frequency activity is the EI. The EI quantifies the ratio between high- and low-

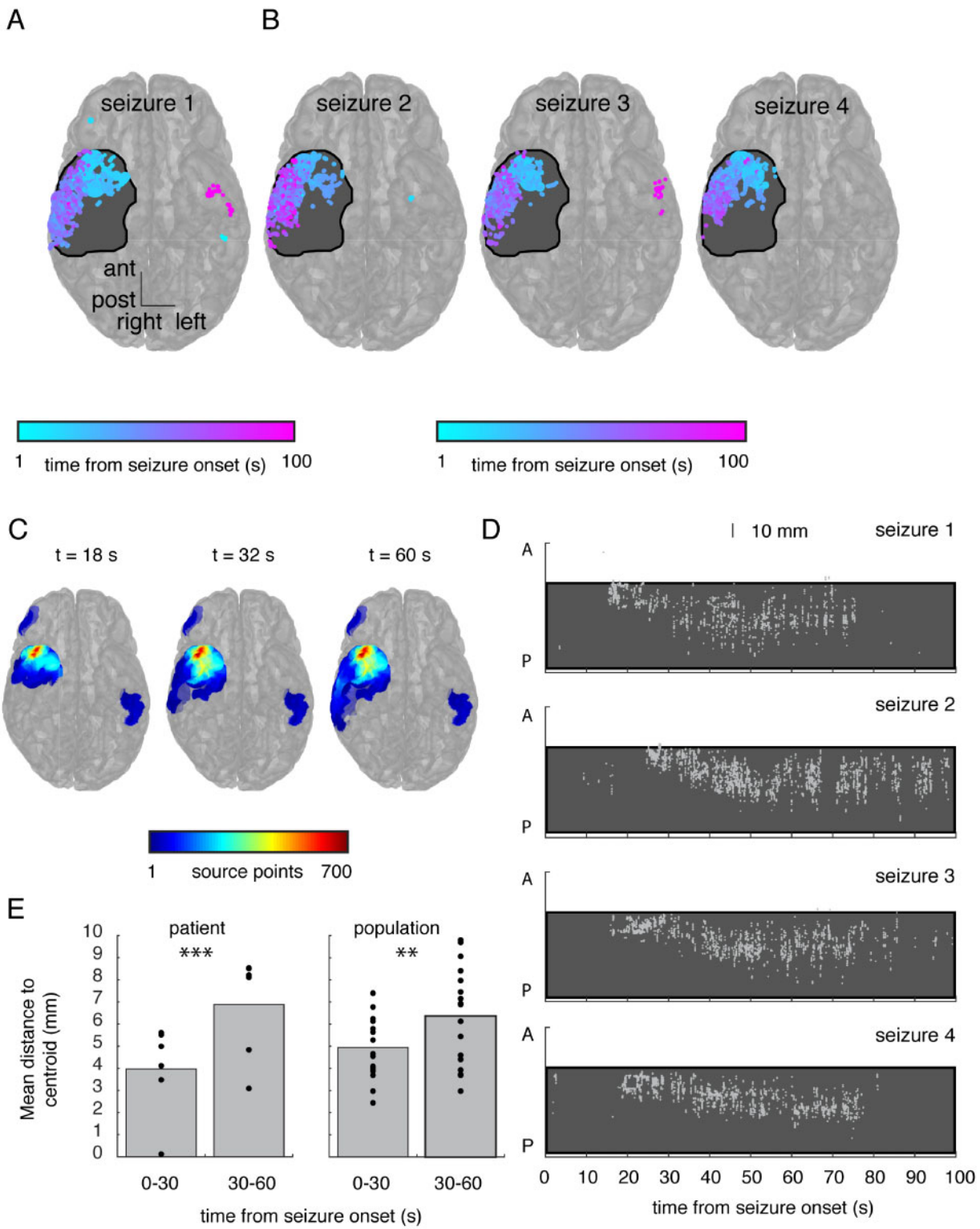

Figure 3 The seizure source moves over long timescales in a stereotyped fashion across seizure events. (**A**) We visualized all locations that were identified as the estimated source of seizure activity throughout this seizure, colour-coded by the time following seizure onset that each location was identified. The size of each point reflects the number of times each individual location was identified as the seizure source. Locations that were identified multiple times are colour-coded by the mean time of their identification. This participant had a subsequent anterior temporal lobectomy (resection region shaded black). For clarity, we collapsed all points along the superior-inferior axis (*right*) to demonstrate the location of each point along the anterior-posterior and left-right dimensions. A transparent brain is shown for reference. The source of the emitted waves initially localizes briefly to the left lateral temporal lobe, then to the right temporal tip, the right lateral temporal cortex, and then again to the left lateral temporal cortex at the end of the seizure. (**B**) Across three additional seizures captured in this participant, the temporal evolution of the seizure source exhibits a similar stereotyped pattern of movement. (**C**) We aggregated discovered source points into regions of interest accumulated over time up to and including three time points in the seizure. Over the course of the seizure, the estimated location of the source migrates from the right anterior subtemporal cortex to the lateral temporal cortex, but rate of localization in these areas does not exceed the high initial rate of source discovery, which localized to

(continued)

frequency energy in the iEEG signal and assigns a high EI to any electrode that demonstrates a high ratio early in the seizure.[1] This metric assigns each electrode an EI, as well as a specific detection time, N_d, when high-frequency activity begins (Supplementary material). When using phase differences to estimate the location of the source, we only consider signals with frequency <12 Hz. We were therefore interested in how well source localization using low-frequency phase differences matches the localization using EI.

In the same example participant as shown in Figs 2 and 3, we averaged the recorded iEEG time series over all electrodes in each subdural strip or grid during a single seizure (Fig. 4A). The average time series data demonstrated that the subtemporal strip electrodes in this participant are the first to exhibit a clear increase in high-amplitude activity. For each electrode, we computed the ratio of high to low-frequency energy at every time point and then computed the average ratio across every electrode in each strip or grid (Fig. 4B; see 'Materials and methods' sections and Supplementary material). High-frequency activity initially emerged in the anterior subtemporal electrodes. The electrode with the highest EI was located within this region and had a detection time of N_d = 1.3 s. About 20 s later, high-amplitude activity emerged in the iEEG time series data in the same location.

We then examined the location of the seizure source estimated using the phase differences in the low-frequency signal. At every time point, we mapped the estimated source point to its closest electrode contact based on geodesic distance. We then counted the number of times each subdural grid or strip contained an electrode that was found to be closest to the estimated seizure source during every second of the seizure (Fig. 4B). Source detection began around 15 s after seizure onset. The closest electrodes to these detected sources were in the grid and the anterior temporal and subtemporal strips, mirroring the emergence of clear high-amplitude activity in these electrodes as well as the location determined by the EI. The detected source then migrated to a location that was nearest to the temporal grid.

We compared the location initially estimated as the source of seizure activity to the location of the electrode exhibiting the highest EI (Fig. 4C). In every seizure in every participant, we identified the first second in which a source location could be estimated and then identified the region of interest containing the most estimated locations during that initial second of localization. We measured the geodesic distance between the centre of the identified region of interest and the location of the electrode with the highest EI. In participants with good outcomes, the regions of interest containing the most estimated source locations during the initial second of localization are more likely to fall within the resection cavity [$\chi^2(1, n = 122) = 37.17$, $P < 0.0001$] and are closer to the electrode with the highest EI than in participants with poor outcomes [89.70 ± 53.43 versus 117.47 ± 47.15; $t(111) = 2.39$, $P = 0.02$] (Supplementary Fig. 5A and B).

We also directly compared the detection time for the electrode with the highest EI to the time when we were first able to estimate the location of any source of seizure activity in all seizures in all participants (Fig. 4D). We again identified the first second during which we were able to estimate the location of the source based on low-frequency phase differences. Relative times to source detection are binned along the horizontal axis, where bins to the right of the vertical axis contain instances in which the first source detection using low-frequency phase occurs after the detection time, N_d.

In most cases, the first seizure source detection occurs within 20 s of N_d. In fact, in many cases, source detection appears to even precede the EI detection time, N_d. We examined this and found several examples in which seizures began with a rhythmic onset rather than low voltage fast activity[2] or in which they began with a herald spike (Supplementary Fig. 5C and F). In seizures with rhythmic onset, EI is not reliable and is typically detected late in a seizure or not at all. Likewise, in seizures that begin with a herald spike, source localization using the observed phase differences in the iEEG electrodes may arise early. In both cases, source detection will appear to precede EI. To confirm this, we removed all rhythmic onset seizures from our analysis and recomputed the time between source localization and EI (Supplementary Fig. 5E).

The estimated seizure source localizes to the resection territory in participants with good outcome

Our data suggest that the phase differences between waves of low-frequency activity detected at the recording electrodes can be used to estimate the location of the source of those waves. An important question is whether widespread high-amplitude rhythmic activity does in fact reflect a focal source. An alternative hypothesis, for instance, would posit that the observed recruitment rhythm instead reflects the recruitment of broad areas of cortex into active seizures. To examine this hypothesis, we measured phase-locked high gamma activity in the iEEG signal, which has recently been shown to serve as a marker for cortical recruitment into ictal activity.[26,27] We found that phase-locked high gamma activity, like our localized seizure source, was likewise focal, and recruitment matched source localization results from the low-frequency phase differences in space and time (Supplementary Fig. 6).

Even with the use of electrographic metrics, there still remains no direct measure of the specific brain region where seizures originate in human patients with epilepsy. However, in some participants it is possible to identify the epileptogenic zone, which represents the region of the brain that, when resected, has led to seizure freedom.[43,44] We divided our participants into those who achieved freedom following surgical resection, and therefore had a good outcome, and those who did not achieve seizure freedom and therefore had a poor outcome. We examined whether the locations estimated to be the source of travelling waves were within or outside the resection territory, which by definition contains the epileptogenic zone in participants with good outcomes and does not contain it in participants with poor outcomes.

In an example participant with a good outcome, we counted the number of times any location in the brain was estimated to be the source of the emitted waves during every second of every seizure and divided those locations into those that fell within the resection cavity and those that were outside of it. On average, across all seizures for this participant, robust source localization

Figure 3 Continued
the anterior temporal lobe. (**D**) The temporal evolution of the location of the estimated seizure source is stereotyped across the four different seizures shown in **A** and **B**. Locations are shown in only the anterior-posterior direction and are collapsed across the superior-inferior and left-right directions. Each grey dot represents a single estimated source location at that time. The region that was subsequently resected in this participant is shaded in black. (**E**) We quantified spatial spread by extracting the mean pairwise distance between estimated source locations during every second of every seizure. We computed the mean spatial spread over the first and second 30 s of each seizure. Across all seizures in this participant, seizure source localization is significantly more diffuse in the second 30 s ($P = 0.0004$; *left*; each dot represents a single seizure). We repeated this analysis in every participant and, averaging across participants, we found a similar difference in spatial spread between the first and second 30 s of seizure ($P = 0.008$; *right*; each dot represents a single patient).

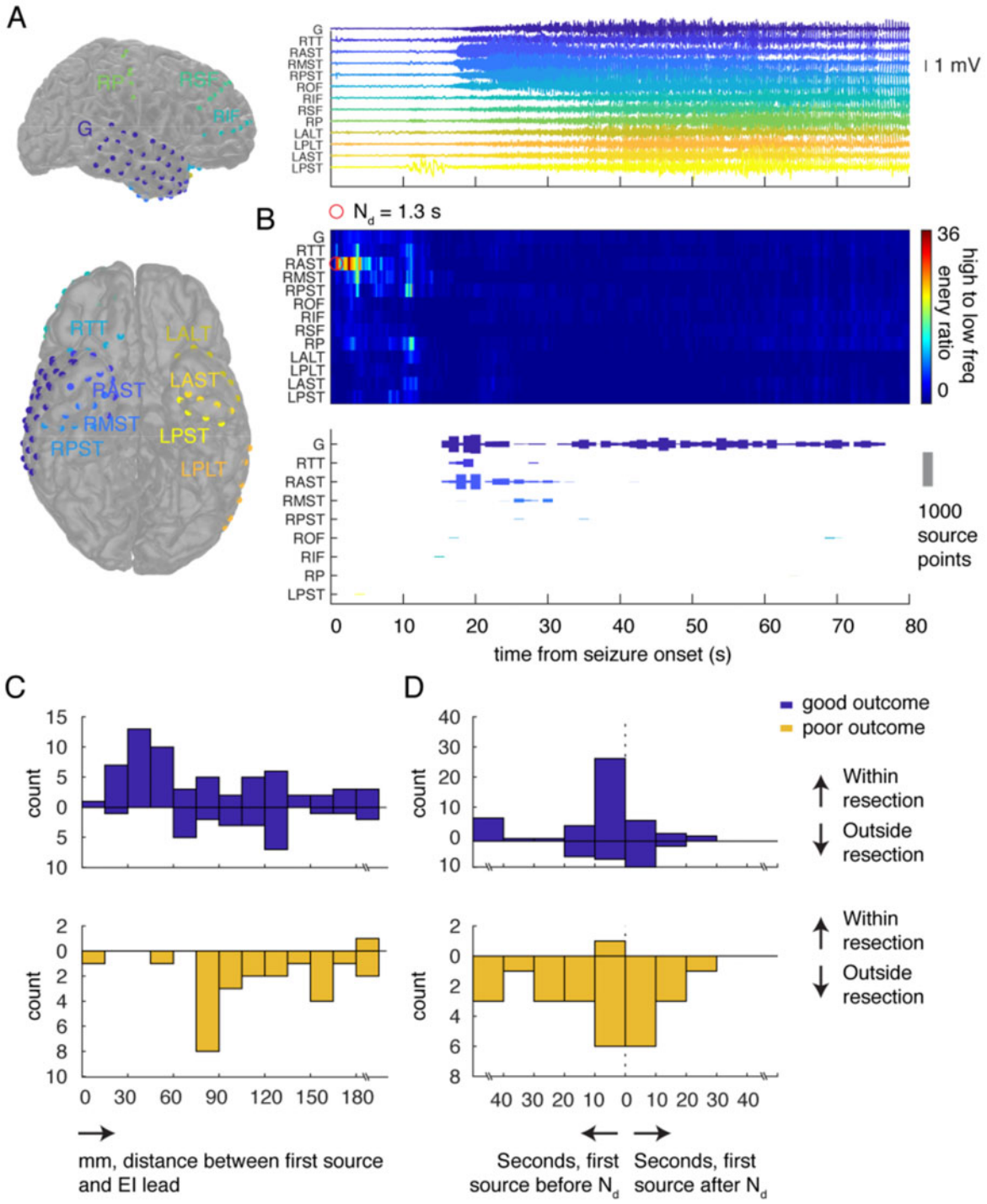

Figure 4 The seizure source emerges from early high-frequency activity. (**A**) All electrodes in an example participant are colour-coded and labelled (*left*). We averaged the iEEG time series across all electrodes in each strip or grid during a single seizure (*right*). (**B**) The ratio of high- to low-frequency energy, averaged for each electrode in each strip or grid for this seizure, increases almost immediately after seizure onset in the anterior subtemporal electrodes, with a detection time N_d of 1.3 s (*top*). In the same seizure, we mapped the estimated location of the seizure source based on low-frequency phase differences to the closest electrode (*bottom*). Each bar represents the number of times the closest electrode to the estimated source location lay within each strip or grid at every second. (**C**) In every seizure in every participant, we identified the first second during which a source location could be estimated, and identified the region of interest containing the most estimated locations during that initial second. We binned the geodesic distances between the centres of the identified regions of interest and the location of the electrode exhibiting the highest EI. (**D**) For every seizure in every participant, we identified the electrode with the highest EI and its detection time, N_d. We computed the relative time between N_d and the first second during which a source location could be estimated based on the low frequency phase differences. We binned these time differences across all seizures in all participants. ALT = anterolateral temporal; AST = anterior subtemporal; G = grid; IF = inferior frontal; L = left; MST = middle subtemporal; OF = orbitofrontal; P = parietal; PLT = posterolateral temporal; PST = posterior subtemporal; R = right; SF = superior frontal; TT = temporal tip.

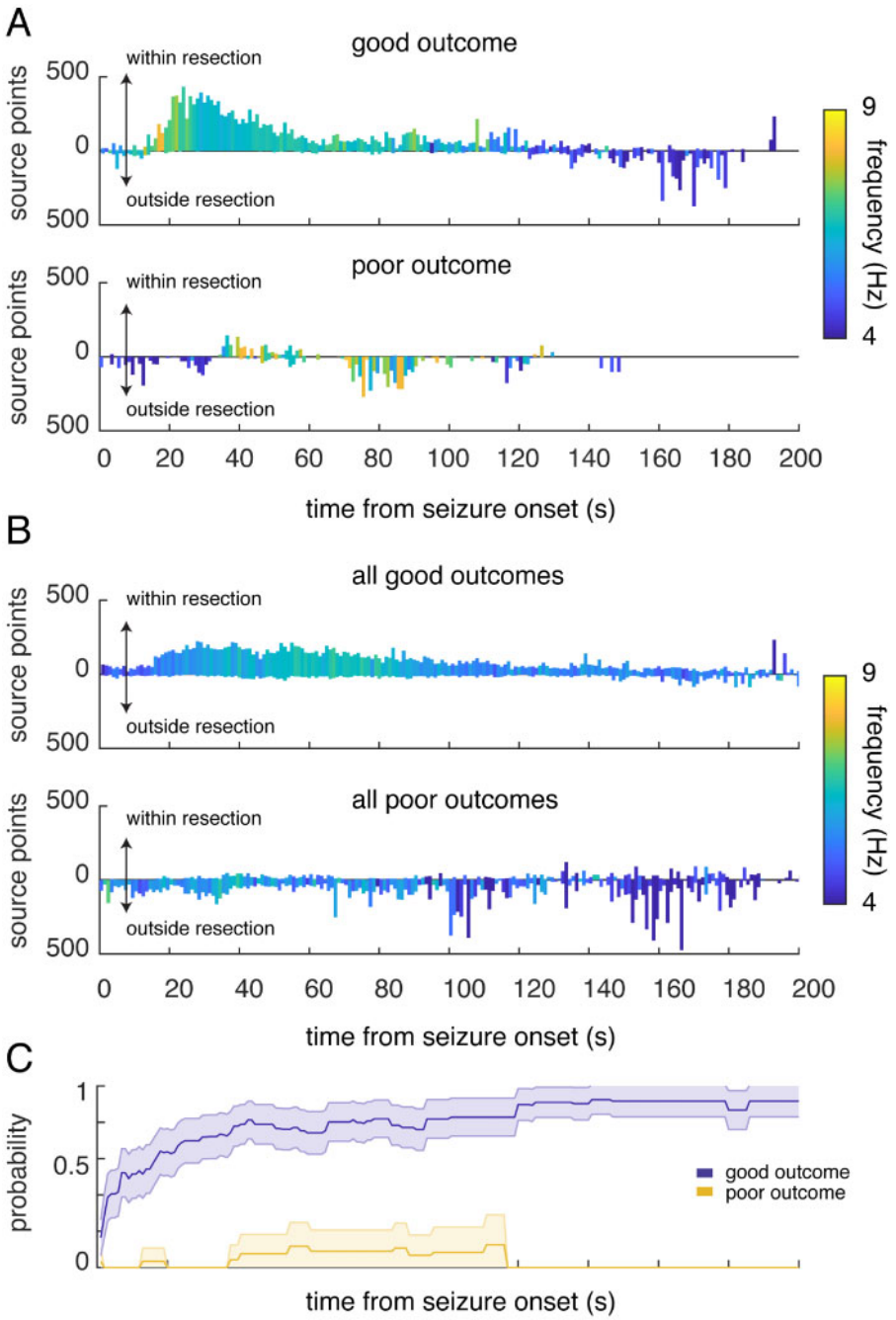

Figure 5 The estimated seizure source localizes to the resection territory in participants with good outcome. (**A**) Source localization in an example participant with a good outcome (*top*) and a poor outcome (*bottom*). For every second and for every seizure, we counted the number of times any location in the brain was estimated to be the source of the emitted waves, and whether those estimated locations fell within or outside the resection territory. Bars represent the average counts per second across all seizures for each participant. The maximum count in any one second is 1000, given the sampling rate of the recorded iEEG trace. Bars are colour-coded by the frequency of the signal detected by the closest electrode to the estimated source at each time point, averaged across seizures. The frequency of the presumed source decreases with seizure progression. (**B**) Counts per second of the estimated locations that fall within and outside the resection territory, averaged across all seizures in each participant and then averaged across all participants with good outcomes (*top*) and with poor outcomes (*bottom*). Bars are colour-coded by the mean frequency detected by the closest electrode to the estimated source, averaged across seizures and then across participants. (**C**) As the seizure progresses in time, we identified the region of interest with the highest peak rate of localization thus far and whether that region of interest is within the resection territory. The likelihood (probability) that the identified region of interest with the highest peak thus far is within the resection territory is computed by aggregating this information across all seizures in each participant. Lines represent this probability, averaged across all participants with good and poor outcomes. Shaded regions represent the standard error of the mean (SEM) across participants.

within the resection cavity occurred relatively early in each seizure (Fig. 5A, top). In a different participant with a poor outcome, however, the number of times during which the estimated source localized to a region within the resection cavity was markedly less (Fig. 5A, bottom). We then examined the number of times any location in the brain was estimated to be the source of the emitted waves at every time point in every seizure in every participant (Supplementary Fig. 1). Averaging across all seizures in each

participant and then across all participants in each group, we found that phase multilateration robustly identifies the estimated location of the source within the resection cavity in those participants with good outcomes but not in those with poor outcomes (Fig. 5B).

Even in participants with good outcomes, the estimated location of the source can fall outside the resection territory at some time points during a seizure. The estimated source, however, clearly localizes more frequently within the resection in these participants. To assess this directly, we calculated the rate of localization for each region of interest, defined as the number of times the estimated source localizes to each region of interest during every second of each seizure. We tracked the progression in time of every seizure in every participant and identified the single region of interest containing the highest peak rate thus far when considering only the time points from the onset of the seizure up to and including each time point of a seizure. Across participants with good outcomes, we found that the region of interest with the highest peak rate identified thus far was increasingly likely to be within the resection territory as the seizure progressed in time (Fig. 5C). On the other hand, in participants with poor outcomes, it was unlikely that the region of interest with the highest peak rate was within the resection territory. Using low-frequency power alone to localize the source did not distinguish between participants with good and poor outcomes (Supplementary Fig. 7A). In addition, when we shuffled the labels for each electrode, we confirmed that source localization did not arise by chance alone (Supplementary Fig. 7B and C).

Discussion

We observed the presence of time delays in wave receipt between electrode pairs during the ictal recruitment rhythm, consistent with a model in which a focal source emits travelling waves of pathologic activity that travel over the cortical sheet. We demonstrated that the sources localized using this model originate from within resected areas in patients with favourable seizure outcomes following surgery and align with standard markers of ictal activity such as the EI and phase-locked high gamma activity. Our results therefore support the emerging hypothesis that, in many brain regions recording rhythmic activity during seizures, this activity may have propagated from a focal source.

A central challenge in the interpretation of iEEG data is determination of the location and timing of seizure origin and spread. Indeed, although surgery is an established treatment for drug-resistant epilepsy, outcomes remain imperfect, particularly in cases where no lesion is seen on preoperative imaging.[45–49] Poor outcomes may be more likely in patients with diffuse, multifocal or progressive underlying pathologies.[48,49] However, reoperation for temporal lobe epilepsy after recurrence improves seizure control relative to the first surgery.[50–54] This suggests that, at least in some patients with an initially poor post-surgical outcome, inaccurate localization of a focal source may have played a role. We address the central challenge of iEEG interpretation by demonstrating that a simple model in which a focal source emits travelling waves can capture properties of the seizure source.

Substantial efforts have recently been invested in the development of neurophysiological metrics for identification of the brain regions involved in seizures. One of the most widely utilized methods is the EI, which identifies electrodes that exhibit an early increase in high-frequency power, which is characteristic of seizure onset.[1] The interpretation of lower-frequency rhythms that emerge later in a seizure is less clear. The traditional interpretation of these rhythms is that they reflect an active seizure in the underlying cortex. Microelectrode recordings, however, have suggested that neuronal activity can remain disorganized even in the presence of such rhythms and only becomes hypersynchronous during and after the passage of the ictal wavefront.[9,13,14,17,26,27] Previous work has shown that phase-locked high gamma activity may be a marker for hypersynchronous neuronal firing and therefore for active seizures. Moreover, regions demonstrating such hypersynchronous activity are spatially confined and migrate slowly across the brain.[26,27] Our data are consistent with these findings, and suggest that in patients with focal epilepsy, seizures may remain more focal for much longer than has previously been understood or suggested by clinical interpretations of iEEG recordings.

Our approach differs considerably from standard neurophysiological measures of seizure onset in that we rely on phase differences in low-frequency activity. Nevertheless, we found robust source detection that is consistent in space and time with the EI in patients with good outcomes. Along with neurophysiologic measures, our model of a focal source of travelling waves, if correct, ought to be corroborated by clinical measures. No direct measure of the seizure source exists in the study of human epilepsy. The current gold standard for establishing the source of seizures is to determine whether an identified location falls within the epileptogenic zone, the brain region that, when resected, leads to seizure freedom.[43,44] We found that our seizure source, as localized by our algorithm, tended to fall within the epileptogenic zone. On the other hand, in patients with poor outcomes, localization usually falls outside of the resection territory.

Our decision to consider low-frequency, high-amplitude rhythms, which usually occur later in the seizure, was based largely on practical factors. Source localization with phase differences is limited by spatial aliasing and requires low-frequency input to avoid ambiguity. However, this practical requirement does not necessarily prevent accurate early source localization. Some recordings begin with low-frequency rhythmic activity, either because seizure onset itself is rhythmic or because initial fast activity is not captured by implanted leads.[2] In these cases, our approach may nonetheless be used for seizure localization, whereas measures of high-frequency activity may be inapplicable. Additionally, some seizures begin with a herald spike, which itself may precede low-voltage fast activity. A herald spike is detectable in our low-frequency band and is often sufficient in and of itself for accurate seizure source localization. It is also important to note that, in contrast with other neurophysiologic methods for source localization, the results of our algorithm are not confined to the locations of implanted leads.

Thus, the simplicity of our model may be one of its strengths. Our model does not incorporate the biophysical properties of the underlying tissue but likewise is also not restricted by these properties. Despite its simplicity, it is sufficient to account for the presence of waves with staggered times of receipt and to reconstruct the source of those waves. This approach is analogous to those used in image processing, for example, in which linear transfer functions may reconstruct an underlying object, such as the tissues that are captured in medical imaging, while remaining agnostic to the physical properties of that object.[55–57] Nonetheless, we acknowledge that the assumptions made under our model—namely, that travelling waves propagate outward in a uniform fashion over the cortical surface—may not reflect reality, possibly at the expense of the model's accuracy. Travelling waves may propagate with a non-uniform speed, or preferentially in some directions, possibly along white matter pathways. Future and more complex iterations of this model may consider the possibility that the seizure source conveys barrages of spiking activity through both local and non-local avenues.

Our data provide support for the hypothesis that the source of pathologic activity can change location over the course of the seizure and is in fact a dynamic entity.[9,26,27] This is consistent with previous *in vivo* and *in vitro* studies of epilepsy that have also suggested that the seizure source is capable of migrating over the course of a seizure.[8,9,15,16,18,22,58] Our data also suggest that in some cases, the seizure source can even split into multiple independent entities, consistent with clinical recordings as well as animal and computational models,[8,9,22] although we cannot exclude the possibility that what appears as two separate sources may in fact reflect a single source delivering travelling waves to distinct cortical sites. Although our data suggest that the seizure source may be dynamic, the mechanisms governing the movement and spread of the seizure source remain undetermined and may vary across patients with different underlying aetiologies and seizure locations. Movement of the seizure source may arise because of progressive recruitment of larger brain regions, from local spread along the cortical sheet or from distant spread along white matter pathways, perhaps even involving subcortical regions.[3,14,23,24,58–60] In each of these cases, the location of the source may appear more diffuse as the direction of propagation of the travelling waves becomes less consistent. Nonetheless, we observed that this migration is relatively stereotyped across seizures within an individual patient. These conserved patterns of migration suggest the existence of preferred pathways of spread, which are likely due to patterns of structural and functional connectivity, as well as to differences in the relative susceptibility of tissues to entrainment into pathological activity.[3,14,17,20]

Such migration can make it difficult to capture patterns of ictal recruitment and propagation in any individual patient. In general, we found more consistent and focal localization earlier in the evolution of seizures, which became more diffuse as the seizure progressed. In patients with good outcomes, localization tended to be more robust and consistent following seizure onset. It is not surprising then that we obtained better surgical outcomes in these patients, who may have had a slower and more contiguous spread of ictal activity.[3,61] One possibility is that in these patients, the seizure focus could lie within cortical areas with stronger local connectivity, which may thus be easier to correctly localize using sparse electrode coverage. On the other hand, in patients with poor outcomes, seizures may exhibit broader or non-contiguous spread patterns, involving brain regions with more widely distributed patterns of connectivity, such as association cortex. Seizures may also arise from multiple locations simultaneously or more diffusely from an epileptogenic network in these patients. In both cases, source detection would be less robust, as we observe here, and accurately identifying the area of seizure onset using sparsely sampled electrodes will remain challenging.

Acknowledgements

We are indebted to all of the patients who have selflessly volunteered their time to participate in this study.

Funding

This work was supported by the Intramural Research Program of the National Institute for Neurological Disorders and Stroke. This work was also made possible through the NIH Medical Research Scholars Program, a public-private partnership supported jointly by the NIH and generous contributions to the Foundation for the NIH from the Doris Duke Charitable Foundation, the American Association for Dental Research, the Colgate-Palmolive Company, Genentech, Elsevier and other private donors.

Competing interests

The authors report no competing interests.

Supplementary material

Supplementary material is available at *Brain* online.

References

1. Bartolomei F, Chauvel P, Wendling F. Epileptogenicity of brain structures in human temporal lobe epilepsy: A quantified study from intracerebral EEG. *Brain*. 2008;131(7):1818–1830.
2. Perucca P, Dubeau F, Gotman J. Intracranial electroencephalographic seizure-onset patterns: Effect of underlying pathology. *Brain*. 2014;137(1):183–196.
3. Martinet LE, Ahmed OJ, Lepage KQ, Cash SS, Kramer MA. Slow spatial recruitment of neocortex during secondarily generalized seizures and its relation to surgical outcome. *J Neurosci*. 2015; 35(25):9477–9490.
4. Kramer MA, Cash SS. Epilepsy as a disorder of cortical network organization. *Neuroscientist*. 2012;18(4):360–372.
5. Zijlmans M, Jacobs J, Kahn YU, Zelmann R, Dubeau F, Gotman J. Ictal and interictal high frequency oscillations in patients with focal epilepsy. *Clin Neurophysiol*. 2011;122(4):664–671.
6. Weiss SA, Alvarado-Rojas C, Bragin A, et al. Ictal onset patterns of local field potentials, high frequency oscillations, and unit activity in human mesial temporal lobe epilepsy. *Epilepsia*. 2016; 57(1):111–121.
7. Jirsch J, Urrestarazu E, LeVan P, Olivier A, Dubeau F, Gotman J. High-frequency oscillations during human focal seizures. *Brain*. 2006;129(6):1593–1608.
8. Proix T, Jirsa VK, Bartolomei F, Guye M, Truccolo W. Predicting the spatiotemporal diversity of seizure propagation and termination in human focal epilepsy. *Nat Commun*. 2018;9(1):1–15.
9. Smith EH, Liou JY, Davis TS, et al. The ictal wavefront is the spatiotemporal source of discharges during spontaneous human seizures. *Nat Commun*. 2016;7:11098.
10. Marsh ED, Peltzer B, Brown IIM, et al. Interictal eeg spikes identify the region of electrographic seizure onset in some, but not all, pediatric epilepsy patients. *Epilepsia*. 2010;51(4):592–601.
11. Behrens E, Zentner J, Van Roost D, Hufnagel A, Elger CE, Schramm J. Subdural and depth electrodes in the presurgical evaluation of epilepsy. *Acta Neurochirurg*. 1994;128(1):84–87.
12. Kim JS, Im CH, Jung YJ, Kim EY, Lee SK, Chung CK. Localization and propagation analysis of ictal source rhythm by electrocorticography. *NeuroImage*. 2010;52(4):1279–1288.
13. Truccolo W, Donoghue JA, Hochberg LR, et al. Single-neuron dynamics in human focal epilepsy. *Nature Neuroscience*. 2011;14(5): 635–641.
14. Schevon CA, Weiss SA, McKhann G Jr, et al. Evidence of an inhibitory restraint of seizure activity in humans. *Nat Commun*. 2012;3:1060.
15. Wenzel M, Hamm JP, Peterka DS, Yuste R. Acute focal seizures start as local synchronizations of neuronal ensembles. *J Neurosci*. 2019;39(43):8562–8575.
16. Trevelyan AJ, Baldeweg T, van Drongelen W, Yuste R, Whittington M. The source of afterdischarge activity in neocortical tonic–clonic epilepsy. *J Neurosci*. 2007;27(49):13513–13519.
17. Wagner FB, Eskandar EN, Cosgrove GR, et al. Microscale spatiotemporal dynamics during neocortical propagation of human focal seizures. *Neuroimage*. 2015;122:114–130.
18. Zhang M, Shivacharan RS, Chiang CC, Gonzalez-Reyes LE, Durand DM. Propagating neural source revealed by Doppler shift of population spiking frequency. *J Neurosci*. 2016;36(12):3495–3505.

19. Gonzalez-Ramirez LR, Ahmed OJ, Cash SS, Wayne CE, Kramer MA. A biologically constrained, mathematical model of cortical wave propagation preceding seizure termination. *PLoS Comput Biol*. 2015;11(2):e1004065.
20. Martinet LE, Fiddyment G, Madsen J, et al. Human seizures couple across spatial scales through travelling wave dynamics. *Nat Commun*. 2017;8(1):14896–14813.
21. Liou J, Smith EH, Bateman LM, et al. Multivariate regression methods for estimating velocity of ictal discharges from human microelectrode recordings. *J Neural Eng*. 2017;14(4):044001.
22. Liou J, Smith EH, Bateman LM, et al. A model for focal seizure onset, propagation, evolution, and progression. *Elife*. 2020;9: e50927.
23. Liu M, Bernhardt BC, Hong SJ, Caldairou B, Bernasconi A, Bernasconi N. The superficial white matter in temporal lobe epilepsy: A key link between structural and functional network disruptions. *Brain*. 2016;139(9):2431–2440.
24. Kim H, Piao Z, Liu P, Bingaman W, Diehl B. Secondary white matter degeneration of the corpus callosum in patients with intractable temporal lobe epilepsy: A diffusion tensor imaging study. *Epilepsy Res*. 2008;81(2-3):136–142.
25. Zhang M, Ladas TP, Qiu C, Shivacharan RS, Gonzalez-Reyes LE, Durand DM. Propagation of epileptiform activity can be independent of synaptic transmission, gap junctions, or diffusion and is consistent with electrical field transmission. *J Neurosci*. 2014;34(4):1409–1419.
26. Weiss SA, Banks GP, McKhann GM Jr, et al. Ictal high frequency oscillations distinguish two types of seizure territories in humans. *Brain*. 2013;136(12):3796–3808.
27. Weiss SA, Lemesiou A, Connors R, et al. Seizure localization using ictal phase-locked high gamma: A retrospective surgical outcome study. *Neurology*. 2015;84(23):2320–2328.
28. Lindén H, Tetzlaff T, Potjans T, et al. Modeling the Spatial Reach of the LFP. Neuron. 2011;72(5):859–872. 10.1016/j.neuron.2011.11.006
29. Toro R, Perron M, Pike B, et al. Brain Size and Folding of the Human Cerebral Cortex. Cerebral Cortex. 2008;18(10):2352–2357. 10.1093/cercor/bhm261
30. Nikitin PV, Martinez R, Ramamurthy S, Leland H, Spiess G, Rao K. Phase based spatial identification of UHF RFID tags. In: *2010 IEEE International Conference on RFID*. IEEE. 2010:102–109.
31. Mo L, Li C, Xie X. Localization of passive UHF RFID tags on the assembly line. In: *2016 International Symposium on Flexible Automation (ISFA)*. IEEE. 2016:141–144.
32. Zhang Y, Amin MG, Kaushik S. Localization and tracking of passive RFID tags based on direction estimation. *Int J Antennas Propag*. 2007;2007:1–9.
33. Hekimian-Williams C, Grant B, Liu X, Zhang Z, Kumar P. Accurate localization of RFID tags using phase difference. In: *2010 IEEE International Conference on RFID*. IEEE. 2010:89–96.
34. Milne J. Earthquakes and other earth movements. D. Appleton and Company; 1886.
35. Zhou H. Rapid three-dimensional hypocentral determination using a master station method. *J Geophys Res Solid Earth*. 1994; 99(B8):15439–15455.
36. Satriano C, Wu YM, Zollo A, Kanamori H. Earthquake early warning: Concepts, methods and physical grounds. *Soil Dyn Earthquake Eng*. 2011;31(2):106–118.
37. Lu C, Dorny C. Ambiguity resolution in self-cohering arrays. *IEEE Trans Antennas Propag*. 1984;32(8):830–835.
38. Engel J Jr, Van Ness P, Rasmussen T, Ojemann L. Outcome with respect to epileptic seizures. *Surg Treat Epilepsies*. 1993;2:609–621.
39. Munoz D, Lara FB, Vargas C, Enriquez-Caldera R. *Position location techniques and applications*. Academic Press; 2009.
40. Matrullo E, De Matteis R, Satriano C, Amoroso O, Zollo A. An improved 1-d seismic velocity model for seismological studies in the Campania–Lucania region (Southern Italy). *Geophys J Int*. 2013;195(1):460–473.
41. Saikia U, Rai S. Seismicity pattern, reference velocity model, and earthquake mechanics of south Indiaseismicity pattern, reference velocity model, and earthquake mechanics of South India. *Bull Seismolog Soc Am*. 2018;108(1):116–129.
42. Boashash B. *T-F signal analysis and processing: A comprehensive reference*. Academic Press; 2015.
43. Rosenow F, Luders H. Presurgical evaluation of epilepsy. *Brain*. 2001;124(9):1683–1700.
44. Luders HO, Najm I, Nair D, Widdess-Walsh P, Bingman W. The epileptogenic zone: General principles. *Epilept Disord*. 2006; 8(Suppl 2):S1–S9.
45. Wiebe S, Blume WT, Girvin JP, Eliasziw M. A randomized, controlled trial of surgery for temporal-lobe epilepsy. *N Engl J Med*. 2001;345(5):311–318.
46. Engel J, McDermott MP, Wiebe S, et al. Early surgical therapy for drug-resistant temporal lobe epilepsy: A randomized trial. *JAMA*. 2012;307(9):922–930.
47. Dwivedi R, Ramanujam B, Chandra PS, et al. Surgery for drug-resistant epilepsy in children. *N Engl J Med*. 2017;377(17):1639–1647.
48. Tellez-Zenteno JF, Ronquillo LH, Moien-Afshari F, Wiebe S. Surgical outcomes in lesional and non-lesional epilepsy: A systematic review and meta-analysis. *Epilepsy Res*. 2010;89310–318. (2):
49. McIntosh AM, Kalnins RM, Mitchell LA, Fabinyi GC, Briellmann RS, Berkovic SF. Temporal lobectomy: Long-term seizure outcome, late recurrence and risks for seizure recurrence. *Brain*. 2004;127(9):2018–2030.
50. Jung R, Aull-Watschinger S, Moser D, et al. Is reoperation an option for patients with temporal lobe epilepsy after failure of surgery? *Seizure*. 2013;22(7):502–506.
51. Krucoff MO, Chan AY, Harward SC, et al. Rates and predictors of success and failure in repeat epilepsy surgery: A meta-analysis and systematic review. *Epilepsia*. 2017;58(12):2133–2142.
52. Grote A, Witt JA, Surges R, et al. A second chance—reoperation in patients with failed surgery for intractable epilepsy: Long-term outcome, neuropsychology and complications. *J Neurol Neurosurg Psychiatry*. 2016;87(4):379–385.
53. Germano IM, Poulin N, Olivier A. Reoperation for recurrent temporal lobe epilepsy. *J Neurosurg*. 1994;81(1):31–36.
54. Awad IA, Nayel MH, Luders H. Second operation after the failure of previous resection for epilepsy. *Neurosurgery*. 1991;28(4): 510–518.
55. Paganin D, Gureyev TE, Pavlov KM, Lewis RA, Kitchen M. Phase retrieval using coherent imaging systems with linear transfer functions. *Optics Commun*. 2004;234(1-6):87–105.
56. Blumich B. Investigation of systematic noise in stochastic linear system analysis. *Rev Sci Instru*. 1986;57(6):1140–1144.
57. Amorim P, Moraes T, Rezende R, Silva J, Pedrini H. Medical imaging for three-dimensional computer-aided models. In: Ovsianikov A, Yoo J, Mironov V, eds. *3D Printing and Biofabrication. Reference Series in Biomedical Engineering*. Springer, Cham; 2016:195–221.
58. Rossi LF, Wykes RC, Kullmann DM, Carandini M. Focal cortical seizures start as standing waves and propagate respecting homotopic connectivity. *Nat Commun*. 2017;8(1):1–11.
59. Wenzel M, Hamm JP, Peterka DS, Yuste R. Reliable and elastic propagation of cortical seizures in vivo. *Cell Rep*. 2017;19(13): 2681–2693.
60. Bernhardt BC, Bernasconi N, Kim H, Bernasconi A. Mapping thalamocortical network pathology in temporal lobe epilepsy. *Neurology*. 2012;78(2):129–136.
61. Kutsy RL. Focal extratemporal epilepsy: Clinical features, EEG patterns, and surgical approach. *J Neurologic Sci*. 1999;166(1):1–15.